Developmental Biology **224,** 42–59 (2000)
doi:10.1006/dbio.2000.9793, available online at http://www.idealibrary.com on IDEAL®

An F-Box/WD40 Repeat-Containing Protein Important for *Dictyostelium* Cell-Type Proportioning, Slug Behaviour, and Culmination

Margaret K. Nelson,* Alexandra Clark,† Tomoaki Abe,‡ Anson Nomura,† Negendra Yadava,† Chanin J. Funair,* Keith A. Jermyn,‡ Sudhasri Mohanty,† Richard A. Firtel,† and Jeffrey G. Williams‡,[1]

**Department of Biology, Allegheny College, Meadville, Pennsylvania 16335; †Section of Cell and Developmental Biology, and The Center for Molecular Genetics, University of California, San Diego, 9500 Gilman Drive, La Jolla, California 92093-0634; and ‡Department of Anatomy and Physiology, University of Dundee, MSI/WTB Complex, Dow Street, Dundee DD1 5EH, United Kingdom*

FbxA is a novel member of a family of proteins that contain an F-box and WD40 repeats and that target specific proteins for degradation via proteasomes. In fruiting bodies formed from cells where the *fbxA* gene is disrupted (*fbxA*$^-$ cells), the spore mass fails to fully ascend the stalk. In addition, *fbxA*$^-$ slugs continue to migrate under environmental conditions where the parental strain immediately forms fruiting bodies. Consistent with this latter behaviour, the development of *fbxA*$^-$ cells is hypersensitive to ammonia, the signaling molecule that regulates the transition from the slug stage to terminal differentiation. The slug comprises an anterior prestalk region and a posterior prespore region and the *fbxA* mRNA is highly enriched in the prestalk cells. The prestalk zone of the slug is further subdivided into an anterior pstA region and a posterior pstO region. In *fbxA*$^-$ slugs the pstO region is reduced in size and the prespore region is proportionately expanded. Our results indicate that FbxA is part of a regulatory pathway that controls cell fate decisions and spatial patterning via regulated protein degradation.

Key Words: Dictyostelium; **WD40 repeat; F-box; ubiquitination; pattern formation; proportioning; differentiation.**

INTRODUCTION

The[1] *Dictyostelium* slug is formed by the aggregation of individual cells but has many of the properties of a multicellular organism. At culmination cells within the slug move and differentiate as either stalk or spore cells. Development is highly regulative. The characteristic 1:4 ratio of stalk to spore cells is maintained over a remarkably wide range of aggregate sizes; as few as 100 cells and as many as 100,000 cells form a correctly proportioned fruiting body. Regulation can also be demonstrated at the slug stage. The slug contains prestalk cells in its anterior one-fifth and prespore cells in the rear four-fifths. If the ratio of these cell types is experimentally altered, by cutting the slug in half, prestalk and prespore cells will each transdifferentiate into the other cell type, thereby reestablishing the correct proportions (Raper, 1940).

In such a highly regulative system, cell-type proportioning must be very tightly controlled; the prestalk cells and prespore cells must "sense" the prestalk-to-prespore ratio and respond appropriately to changes in it. This capacity implies the existence of diffusible signals that direct cellular differentiation. The two best characterised signals that could regulate this process are DIF, a chlorinated hexaphenone, and cAMP (reviewed by Brown *et al.*, 1997; Kay, 1997). Cells aggregate together using extracellular cAMP signals but, in addition to acting as a chemoattractant, cAMP also induces prespore differentiation. DIF acts antagonistically to cAMP, to induce prestalk differentiation and inhibit prespore cell differentiation. Once a mound is formed, the prestalk cells sort to the apex where they form a nipple-shaped tip. The tipped mound transforms into a

[1] To whom correspondence requests should be addressed.

0012-1606/00 $35.00

cylindrical standing slug and, under the environmental conditions likely to exist below the forest floor (high humidity, darkness, and high ionic strength), the slug falls over and enters a migratory stage.

The slug is phototactic and thermotactic and these sensitivities direct it to a suitable environment for culmination. Under certain laboratory conditions, the migratory slug phase is omitted and development then takes 24 h. Ammonia, which is produced during development as a result of protein catabolism, is believed to act as the regulator for entry into culmination; high levels of ammonia inhibit culmination and depletion of ammonia is sufficient to trigger culmination (Schindler and Sussman, 1977). A number of mutants that persist as slugs under conditions that would normally induce culmination have been shown to be hypersensitive to the inhibitory effects of ammonia (Gee *et al.*, 1994; Newell and Ross, 1982).

Most aspects of slug behaviour seem to be under the control of the slug tip. When the tip from one slug is grafted onto the flank of another slug the donor tip recruits a cohort of prespore cells from the recipient slug (Raper, 1940). Also, the duration of slug migration is determined by the tip (Fukuzawa *et al.*, 1997; Smith and Williams, 1980) and the tip is the light sensor for phototaxis (Francis, 1964). There is a molecular marker for the tip region that is derived from the *ecmA* gene (Early *et al.*, 1993). *ecmA* encodes an extracellular matrix protein and it is expressed throughout the prestalk region. *ecmA* is also expressed in the anterior-like cells (ALC), a population of cells with the characteristics of prestalk cells that lie scattered throughout the prespore region. The promoter of the *ecmA* gene is modular. Prestalk cells that utilise the region proximal to the cap site (the *ecmO* region) are known as pstO cells, while those that utilise the distal region (the *ecmA* region) are called pstA cells. Many of the ALC utilise the *ecmO* region, while very few utilise the *ecmA* region. pstA cells are found in the front one-third to one-half of the prestalk region, while pstO cells occupy the remainder of the prestalk region.

Because the pstA cells occupy the front of the prestalk zone, they probably correspond to the functionally defined tip and genetic evidence supports this notion (Fukuzawa *et al.*, 1997). The tip cells are, however, a constantly changing population, because there is a cellular flow within the migrating slug (Abe *et al.*, 1994). There is a cone of cells in the front of the prestalk region, the pstAB cells, identified by the fact that they express both *ecmA* and a closely related extracellular matrix protein, *ecmB*. During slug migration there is a sporadic shedding of the entire cone of pstAB cells from the tip (Sternfeld, 1992). The pstAB cells lost from the prestalk region are then replaced as follows: a subset of pstA cells activates *ecmB* and so becomes pstAB cells, pstO cells differentiate into pstA cells and move forward into the tip, ALCs move from the prespore region into the pstO region, and prespore cells transdifferentiate to replenish the ALC population. As a result, the relative proportions of pstA, pstO, and prespore cells remain fairly constant despite the cell losses associated with migration.

At culmination the slug sits on end and a pattern of morphogenetic movement is initiated within the prestalk region, whereby the pstA cells move downward toward the base. As the pstA cells start their downward movement, they activate expression of the *ecmB* gene. They do so using promoter elements proximal to the *ecmB* cap site (Ceccarelli *et al.*, 1991). These cells synthesise around themselves a matrix known as the stalk tube (for convenience, we will term cells within the stalk tube ST cells). Entry into the stalk tube is sequential and once the pstA cells have all become ST cells they are followed into the stalk tube by the pstO cells. Some of the pstO cells activate expression of the *ecmB* gene before they enter the stalk tube and this defines them as "upper cup" cells (UC cells; Ceccarelli *et al.*, 1991). There are two additional, very closely related populations of *ecmB*-expressing cells: the "lower cup" (LC) and the basal disc (BD) cells (*N.B.* The names upper cup and lower cup derive from the position of these cells in the final culminant: at the apex and base of the spore mass, respectively.).

One very powerful approach to study a pattern formation process is to isolate mutants that disrupt normal development. We have identified a mutant that produces aberrant fruiting bodies, that remains at the slug stage under conditions where the parental strain culminates, and that is aberrant in cell-type proportioning. Because the mutant was made using insertional mutagenesis (Kuspa and Loomis, 1992), we were able to isolate and characterise the disrupted gene. This gene, *fbxA*, plays a key role in regulating cell fate decisions. Since the FbxA protein contains an F-box and WD40 repeats, which direct proteins to be degraded by the ubiquitin/proteasome pathway, it is probable that FbxA regulates developmental fate via targeted protein degradation.

MATERIALS AND METHODS

Cells and Growth Conditions

Cells were cultured at 22°C in either shaking flasks or in tissue culture dishes. *DH1* cells, which are uracil auxotrophs, were grown in FM medium (Gibco/BRL) supplemented with uracil at 20 μg/ml. REMI mutants were initially selected in FM lacking uracil (Kuspa and Loomis, 1992). Following cloning of individual Ura+ mutant strains, cells were maintained in HL5 medium (Watts and Ashworth, 1970). Ax2 and KAx3 cells were grown in HL5 medium. *fbxA*$^-$ mutants created in the Ax2 or KAx3 background were initially selected at 10 μg/ml Blasticidin S (ICN/Flow). Following cloning of individual integrants and confirmation of the expected integration event by a Southern transfer, the mutants were maintained in HL5 without selection. Strains transformed with *lacZ* reporter plasmids or the *actin15-fbxA-FLAG* construct were selected in HL5 containing 20 μg/ml G418 (geneticin; Gibco/BRL). In order to select for cells expressing FbxA-FLAG at higher levels, aliquots of the *actin15-fbxA-FLAG* transformants were transferred to HL5 containing 100 μg/ml G418.

Developmental Conditions

For standard developmental assays, cells were harvested from axenic medium, washed twice in KK2 phosphate buffer (16.5 mM KH_2PO_4, 3.8 mM K_2HPO_4, pH 6.2), resuspended at 10^8 cells/ml in KK2, and plated at a density of approximately 2.5×10^6 cells/cm^2 (unless otherwise noted) on either 2% water agar plates or on Millipore 0.45-μm nitrocellulose filters atop a filter pad soaked in KK2. Developing cells were incubated at 22°C in either overhead or unidirectional light, as appropriate for a given experiment.

For synergy experiments, each population of cells was washed as described above and resuspended in KK2 at a density of 1×10^8 cells/ml. Mixtures were prepared containing 10% (v/v) marked cells and 90% (v/v) unmarked cells and plated on either filters or agar, as appropriate.

In the case of the slugger assay in which *fbxA1*$^-$ was originally identified, LPS (lower pad solution, 29.2 mM KH_2PO_4, 1.07 mM Na_2HPO_4, pH 6.4) was substituted for KK2 buffer and cells were plated on filters, followed by incubation for 40 h in unidirectional light. Mutants were classified as sluggers if they showed evidence of slug migration (either the continued presence of slugs after 40 h of development or the culminants located outside the original region of cell deposition).

To compare the sensitivity of parental and *fbxA*$^-$ mutant strains to ammonia, cells were harvested from axenic culture and washed twice in 25 mM MES, pH 6.2. During the second wash step, the cells were split into multiple aliquots, each of which was resuspended at a density of 2×10^8 cells/ml (*fbxA1*$^-$) or 1×10^8 cells/ml (*fbxA2*$^-$) in 25 mM MES, pH 6.2, containing a given concentration of NH_4Cl (0, 5, 10, 20, 40, 60, or 75 mM). Filters and pads, presoaked in the same series of NH_4Cl/MES solutions, were also prepared. Cells were plated on the corresponding filter and pad at a density of 5.0×10^6 cells/cm^2 (*fbxA1*$^-$) or 2.5×10^6 cells/cm^2 (*fbxA2*$^-$) and monitored over the course of development.

Molecular Analysis

Genomic DNA flanking the site of REMI insertion in *DH1* was recovered by digesting genomic DNA from the mutant strain with a restriction enzyme (*Bcl*I or *Spe*I) that does not cut in the plasmid used for insertional mutagenesis. The resulting DNA fragments were circularized via ligation and transformed into bacteria. In order to demonstrate that the mutant phenotype was a consequence of the insertion event, DNA prepared from the rescued plasmids was linearized with the enzyme used for the initial excision and retransformed into *DH1* cells, using the standard conditions for REMI mutagenesis (Kuspa and Loomis, 1992) but omitting any restriction enzyme. Ura+ transformants were screened for developmental morphology. Southern analysis of DNA prepared from transformant clones was used to confirm that recapitulation of the original insertion event via homologous recombination reproduced the original phenotype.

The sequence of the *fbxA* gene was derived largely from analysis of genomic DNA (contained either in the plasmids described above or in MC1, a plasmid produced by digestion of genomic DNA with *Cla*I, which cuts once in the insertion plasmid). In order to sequence across the site of insertion and to verify the position of the 5′ noncoding region, PCR was used to amplify fragments from a *Dictyostelium* cDNA library. Primers that anneal either 68 bp downstream of the putative ATG translation start site or 51 bp upstream of the insertion site were used in combination with primers that anneal in the cDNA backbone. The resulting fragments were treated with *Bam*HI and *Eco*RI (which cut at sites that were engineered into the PCR primers) and inserted into the polylinker region of Bluescript SK+ (Stratagene). The T3 and T7 primers, which hybridise to areas flanking the polylinker region, were used to sequence the plasmids. The plasmid derived from the 5′ region (318 MN) was shown to contain the predicted coding sequence plus approximately 155 bp of upstream DNA, with stop codons in all reading frames. This sequence matched that obtained from analysis of genomic DNA. Similarly, the plasmid derived from the 3′ region of the gene (319 MN) confirmed that the DNA sequence predicted by sequencing outward from the site of insertion in rescue plasmid is, in fact, contiguous in the native gene. DNA sequencing reactions were carried out using either ^{35}S-dATP and the Pharmacia T7 sequencing kit or the Applied Biosystems *Taq* dye primer cycle sequencing kit and an ABI377 automated sequencer.

The template for the probe used for hybridisation with the YAC library was a 0.9-kbp *Bcl*I/*Bam*HI fragment (comparable to the *Bcl*I/*Bam*HI fragment in the C-terminal region of the MC1 insert excised from one of the orignal *fbxA1*$^-$ rescue plasmids (pMB3, produced by digestion of genomic DNA with *Bcl*I; see above). The plasmid Bsr▽1, which was used to create the mutant *fbxA2-*, was constructed as follows. MC1 (see above) was digested with *Bcl*I to remove a 3.07-kbp region of DNA (containing 111 bp of 5′ noncoding sequence and the coding region for the first 944 amino acids of FbxA). The remaining backbone was ligated with a 1.5-kbp *Bam*HI fragment containing a Blasticidin-resistance gene under the control of the *actin15* promoter (Sutoh, 1993) to produce Bsr▽1. A second disruption plasmid, Bsr▽2, was used to create the *fbxA3*$^-$ mutant. Bsr▽2 was made by inserting a blunt-ended version of the same Blasticidin-resistance cassette into a unique *Hin*cII site near the centre of the FbxA coding region. The plasmid 316 MN was used as the template for riboprobe preparation for *in situ* analysis of the *fbxA* expression pattern. 316 MN consists of a 175-bp fragment PCR amplified from the extreme 5′ region of the FbxA coding region cloned into the *Eco*RI and *Bam*HI sites of Bluescript SK+ (Stratagene).

The *actin15*-FbxA-FLAG construct was assembled in two steps. First, two oligos were synthesized (MN Fl upper, 5′-AAT TCA GAT TAT AAG GAT GAT GAC GAT AAG TAA GAT CTA–3′; and MN Fl lower, 5′-A GCT TAG ATC TTA CTT ATC CTG CTA ATC CTT ATA ATC GT-3′) and annealed to produce a double-stranded DNA fragment with *Eco*RI and *Hin*dIII cohesive ends that encodes the FLAG epitope tag (Sigma-Aldrich) and a stop codon. This fragment was inserted between the *actin15* promoter and *actin8* terminator sequences in the vector pDEX-RH (Faix *et al.*, 1990) to produce the intermediate plasmid 321 MN. A 3.9-kbp fragment was produced via PCR, using MC1 as a template and primers designed to amplify the entire FbxA coding sequence, with the exception of the stop codon. These primers also introduced an *Eco*RI site at each end of the fragment. This fragment and the plasmid 321 MN were each digested with *Eco*RI and then ligated together. Constructs containing inserts in the appropriate orientation (as determined by restriction enzyme digestion) were subjected to sequence analysis to confirm that an in-frame fusion had been produced. The resulting fusion protein adds 11 amino acids to the extreme C-terminus of FbxA (KNSDYKDDDDK), immediately upstream of the stop codon. Three individual plasmids (F2, F3, and F5) that contained the desired fusion construct were introduced separately into both Ax2 and *fbxA2*$^-$ cells via calcium phosphate precipitation (Nellen *et al.*, 1984). All three sets of fbxA2$^-$ transformants produce fruiting bodies, containing normal stalk and spore cells, but the morphology of the structures is somewhat

imperfect, presumably because expression is driven by the semi-constitutive actin 15 promoter. Because the morphology of F3 transformant fruiting bodies was particularly poor, the F2 and F5 transformants of Ax2 were used in all further analyses.

Creation of the fbxA2⁻ and fbxA3⁻ Mutant Strains

For the creation of the *fbxA2⁻* mutant, the Bsr▽1 disruption plasmid was first digested with *Cla*I and *Bam*HI. This separates the vector backbone from a fragment containing the Blasticidin cassette flanked by 1.1 kbp of DNA from the upstream promoter region of *fbxA* and 0.9 kbp of FbxA coding sequence. Similarly, the Bsr▽2 disruption plasmid was cut with *Acc*I and *Nde*I to release the fragment used in creation of *fbxA3⁻*. In both cases, the digestion mixture was phenol/chloroform-extracted, ethanol-precipitated, and resuspended in sterile water. Ten micrograms of DNA was introduced into Ax2 cells (*fbxA2⁻*) or KAx3 cells (*fbxA3⁻*) via electroporation, using the same conditions as those for REMI mutagenesis (Kuspa and Loomis, 1992) but in the absence of any accompanying restriction enzyme. Blasticidin-resistant transformants were screened for developmental morphology. Southern analysis of DNA prepared from transformant clones with a mutant phenotype was used to confirm that the expected homologous recombination event had occurred. Parallel analysis of DNA from phenotypically normal transformants showed no evidence of disruption of the *fbxA* locus.

In Situ Hybridisation Analysis

For analysis of the *fbxA* expression pattern, a dUTP digoxigenin riboprobe was prepared using linearized 316 MN as a template and a DIG RNA labeling kit (Boehringer Mannheim 1175025). 316 MN was linearized with *Eco*RI and transcribed from the T3 promoter to produce an antisense probe; the sense probe was transcribed from the T7 promoter following linearization of the template DNA with *Bam*HI. The probes were partially hydrolysed with 0.1 M carbonate, pH 10, for 20 min at 65°C, as recommended by O'Neill and Bier (1994). Sample preparation and hybridisation procedures were those described by Escalante and Loomis (1995), modified for use with riboprobes as later suggested by the authors (personal communication) by a carbonate treatment of the probe, prehybridisation, and hybridisation at 50°C, and a final wash in 0.1× SSC. EcmA gene expression was analysed using a 800-bp probe from within the ecmA coding sequence.

Western Blot Analysis of actin-FbxA-FLAG Transformants

Untransformed Ax2 cells and Ax2 cells transformed with F2 or F5 (see above) were allowed to develop for 6.5 h on water agar in overhead light. The resulting loose mounds were washed off the plate using KK2, harvested via centrifugation, resuspended in 20 mM potassium phosphate buffer, pH 7.0, and disaggregated via passage through a 23-gauge needle. The cells were then pelleted and resuspended directly in 5× Laemmli sample buffer at a concentration of 6.7×10^7 cells/ml. Cells (1×10^6) were loaded per lane on a 7% SDS-PAGE gel. Following electrophoresis the gel was blotted to Hybond-C membrane (Amersham). The resulting blot was blocked for 1 h at 25°C in 10% milk (w/v) in PBST (PBS + 0.05%, v/v, Triton X-100) and incubated overnight at 4°C with a 1:500 dilution (final concentration 2 μg/ml) of affinity-purified polyclonal rabbit anti-FLAG antibody (Zymed) in fresh blocking solution. The following day the blot was washed (3 × 15 min) in PBST, incubated for 1 h at 25°C with a 1:1000 dilution of HRP-conjugated goat anti-rabbit (Bio-Rad) in 5% milk (w/v) in PBST, washed again, and incubated for 1 min at 25°C with ECL detection reagents (Amersham). The signal was detected via exposure of the blot to X-ray film.

Indirect Immunofluorescence

For Mud1 (Krefft *et al.*, 1983) staining, first fingers or slugs, as appropriate, were disaggregated as described for the Western blot analysis. Disaggregated cells were dispensed onto poly-L-lysine coated slides and allowed to settle for 10 min at 25°C. The buffer solution was removed and the cells were fixed for 10 min in 100% MeOH at 25°C. Following fixation, the methanol was allowed to evaporate from the surface of the slide. The cells were then incubated in a moist chamber with 2 μg/ml Mud1 antibody (gift of M. Krefft) in PBS for 4 h at 25°C, washed, then incubated with 2 μg/ml FITC goat anti-mouse (purchased from Biosource International and preadsorbed by incubation with *Dictyostelium* cells) in PBS for 4 h at 25°C, washed again, and finally sealed under coverslips. The samples were examined under an Leica DM-RBE fluorescence microscope, using a 40× objective. Fields were chosen at random and the percentage of total cells stained was determined. Approximately 2000 total cells were counted for each strain at a given developmental stage.

In the case of staining with antibody directed against spore coat proteins (Hayashi and Takeuchi, 1976) first fingers were carefully transferred from 2% water agar to poly-L-lysine-coated slides and fixed in 100% methanol at 25°C. The fixed structures were incubated overnight at 4°C with a 1:1000 antibody dilution in PBS, washed, incubated with 1:1000 Texas red conjugated goat anti-rabbit (purchased from Molecular Probes and preadsorbed by incubation with *Dictyostelium* cells) in PBS for 4 h at 25°C, washed again, sealed under a coverslip, and and examined using a Leica TCS-NT confocal microscope.

β-Galactosidase Staining

Ax2 and *fbxA2⁻* cells were transformed with a series of cell type-specific *lacZ* reporter plasmids and transformants were grown and developed as described above. Fixation, washing, and staining procedures were those of Dingerman *et al.* (1989). Staining times depended on the *lacZ* construct in question and the particular experiment. However, for any one stage of development in a given experiment, Ax2 and *fbxA2⁻* transformants were incubated for the same length of time.

RESULTS

Isolation of the fbxA1⁻ Mutant and the fbxA Gene

Developmental mutants, produced using REMI (Restriction Enzyme-Mediated Integration; Kuspa and Loomis, 1992), were screened for culmination abnormalities. Depending upon the precise developmental conditions, the *fbxA1⁻* mutant forms aberrant fruiting bodies, remains as a migratory slug under conditions where the parental strain enters culmination, or arrests at the mound stage (data not shown). When analysing REMI mutants, there is always a risk that the observed phenotype results from DNA damage

at a site other than the vector insertion site. The *fbxA* gene was therefore cloned by recovery of the DNA flanking the site of plasmid insertion in the REMI mutant. To demonstrate that the mutant phenotype is a consequence of the insertion event, DNA prepared from the rescued plasmid was linearized with the restriction enzyme used for the initial excision and retransformed into *DH1* cells. Southern blot analysis of DNA prepared from transformant clones showed that recapitulation of the original insertion event had occurred in a fraction of the transformants. The phenotypes observed in these re-disruptants were the same as those of the original REMI isolate and Southern blot analysis demonstrated a direct correlation between strains with the mutant phenotype and a disruption of the gene (data not shown).

The full sequence of the *fbxA* gene was determined, largely via analysis of genomic DNA. However, cDNA clones were used to sequence across the insertion site and to verify the positions of the 5′ noncoding region and the single intron, which lies near the 5′ end of the gene. Hybridisation of an *fbxA* probe with a YAC library shows that *fbxA* maps to chromosome 2 (A. Kuspa, personal communication; Kuspa and Loomis, 1996). *fbxA* is predicted to encode a protein, FbxA (for "F-box A"), of 142 kDa. The amino acid sequence of FbxA is shown in Fig. 1A. The protein contains an F-box and five WD40 repeats, which are located C-terminal to the F-box (Fig. 1). F-Boxes mediate interaction of proteins with the ubiquitination machinery (Patton *et al.*, 1998; Maniatis, 1999) and are often found associated with WD40 repeats. WD40 repeats have been identified in a wide variety of eukaryotic proteins and are thought to mediate protein-protein interactions (Neer *et al.*, 1994). FbxA contains several poly-Gln, poly-Thr, and poly-Asn tracts derived from poly AAC runs in the coding sequence, a feature common to many *Dictyostelium* genes (Shaw *et al.*, 1989).

fbxA Is a Developmentally Regulated Gene with a Transcript That Is Enriched in Prestalk Cells

When analysed by Northern blot hybridisation, the *fbxA* mRNA is undetectable in vegetative cells, peaks at approximately 14 h (first finger/slug stage), and drops in abundance by 18 h (Mexican Hat stage; data not shown). *In situ* analysis of whole-mount preparations shows that *fbxA* mRNA is highly enriched in prestalk cells. There is strong staining in the prestalk zone of all tipped aggregates (data not shown) and all slugs (Fig. 2A) and in the rear of a proportion of slugs (Fig. 2A, lower of the two slugs; *N.B.*, this is the rearguard region, a prestalk cell population that is present in some but not all slugs and that forms part of the outer basal disc at culmination; Jermyn and Williams, 1991). No staining is observed in *fbxA*$^-$ slugs or when a control, sense probe is used. (Figs. 2B and 2C). We could not distinguish any signal above background when preculminants and culminants were examined (data not shown).

Creation of New fbxA Null Alleles and Phenotypic Characterisation

The original *fbxA1*$^-$ mutation results from plasmid insertion at a site very near the predicted C-terminus of the FbxA protein (Fig. 1A). Hence it seemed possible that a partially functional protein might be produced. Therefore, before analysing FbxA function in detail, two new disruption constructs were produced and analysed in two different strains. In one plasmid (Bsr▽1) a 3.07-kb region encompassing 111 nucleotides of upstream sequence, the ATG start codon, and 944 amino acids of FbxA was replaced with a cassette encoding resistance to Blasticidin. Following digestion with *Cla*I and *Bam*HI, Bsr▽1 was transformed into strain Ax2 to yield strain *fbxA2*$^-$. In plasmid Bsr▽2, a blasticidin resistance cassette was inserted at a unique *Hinc*II site near the centre of *fbxA*. Bsr▽2 was cut with *Acc*I and *Nde*I and transformed into KAx3 to produce strain *fbxA3*$^-$. In both cases disruption of the *fbxA* gene was confirmed by Southern blot analysis (data not shown).

There are minor differences among *fbxA1*$^-$, *fbxA2*$^-$, and *fbxA3*$^-$, almost certainly arising from the fact that the parent strains of *fbxA1*$^-$ (DH1), *fbxA2*$^-$ (Ax2), and *fbxA3*$^-$ (KAx3) differ in their precise developmental characteristics, but the general properties of the mutants are very similar. All three mutant strains form aberrant culminants when developed in overhead light but the proportion of aggregates that develop into culminants is highest with *fbxA2*$^-$; *fbxA1*$^-$ and *fbxA3*$^-$ show some tendency to arrest as mounds, particularly when developed at low cell densities (data not shown). All three strains are much more likely to remain as slugs under developmental conditions where the parent strain enters culmination. This defect is best illustrated when cells are developed on nitrocellulose filters. Under these conditions, parental cells culminate without a migratory slug stage (Fig. 3A) but *fbxA*$^-$ cells migrate as slugs for many hours before some, but not all, of the slugs eventually form aberrant culminants (Figs. 3B and 3C). Squashes of the culminants reveal a normal stalk tube, vacuolated stalk cells, and refractile spores that are detergent resistant (Fig. 3D and data not shown). When *fbxA*$^-$ slugs are exposed to overhead light (which triggers culmination in wild-type strains), some of the *fbxA*$^-$ null slugs culminate, while others form amorphous mounds (marked with arrowheads in Fig. 3E). Since the three strains show such similar properties, we will henceforth simply refer to them as *fbxA*$^-$ mutants.

fbxA$^-$ *Development Is Hypersensitive to Ammonia*

Since *fbxA*$^-$ slugs tend to migrate for extended periods of time compared to parental strains (this is termed a "slugger" phenotype), and several previously described slugger mutants have been shown to be ammonia hypersensitive (Gee *et al.*, 1994), we determined whether *fbxA*$^-$ mutants also display this property. Parental and mutant cells were developed in the presence of increasing concentrations of ammonium chloride. *fbxA*$^-$ cells are much more sensitive

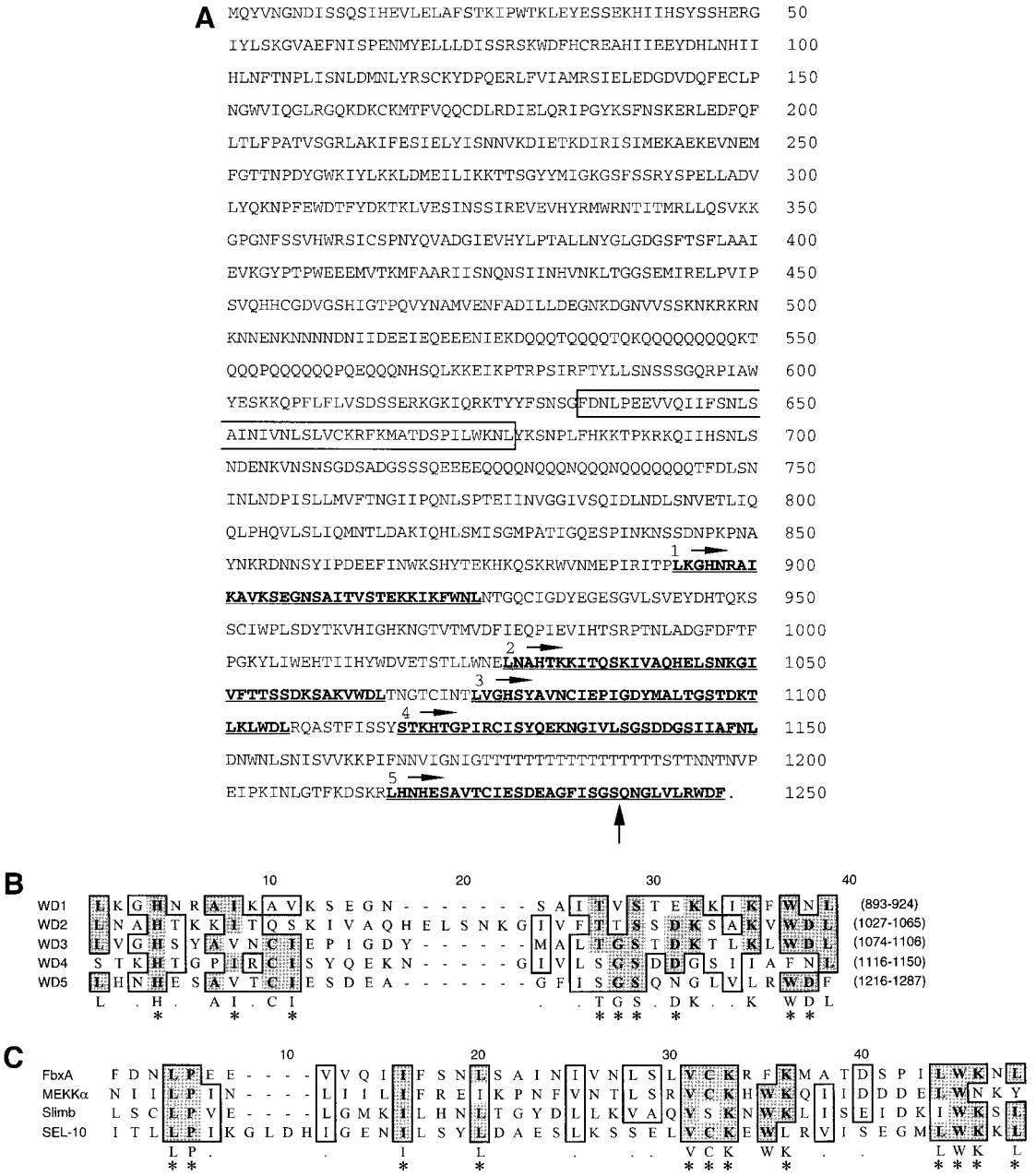

FIG. 1. The structure of the FbxA protein. (A) Predicted amino acid sequence of FbxA. The F-box is enclosed by a box. The five WD40 repeats are in bold and underlined and numbered. The beginning of each WD40 repeat is marked by a horizontal arrow. The vertical arrow between residues 1237 and 1238 marks the site of plasmid insertion in *fbxA1*$^{-}$. (B) Alignment of FbxA's WD40 repeats. The five WD40 repeats from FbxA were aligned using the program CLUSTAL W. The resulting consensus is shown in the line immediately below the repeats. Letters and dots indicate exact matches and related residues, respectively, in >50% of the cases. Asterisks mark places where CLUSTAL's consensus matches those suggested for WD40 repeats (Neer *et al.*, 1994). The residue numbers for each repeat are shown to the right. (C) Alignment of F-box regions from several F-box/WD40 proteins. F-boxes from FbxA (residues 634–677), *Dictyostelium* MEKKα, *Drosophila* Slimb, and *C. elegans* SEL-10 were aligned using CLUSTAL W. Coordinates for the F-boxes are based on the consensus in the review by Patton *et al.* (1998). The resulting consensus is shown in the line immediately below the repeats. Letters and dots indicate exact matches and related residues, respectively, in >50% of the cases. Asterisks mark places where CLUSTAL's consensus matches those suggested by Patton *et al.* (1998). The F-box from FbxA shows exact matches to 26 of the 33 residues specified by the Patton consensus. In 6 of the remaining 7 cases, the residue in FbxA matches that found in at least one other F-box protein.

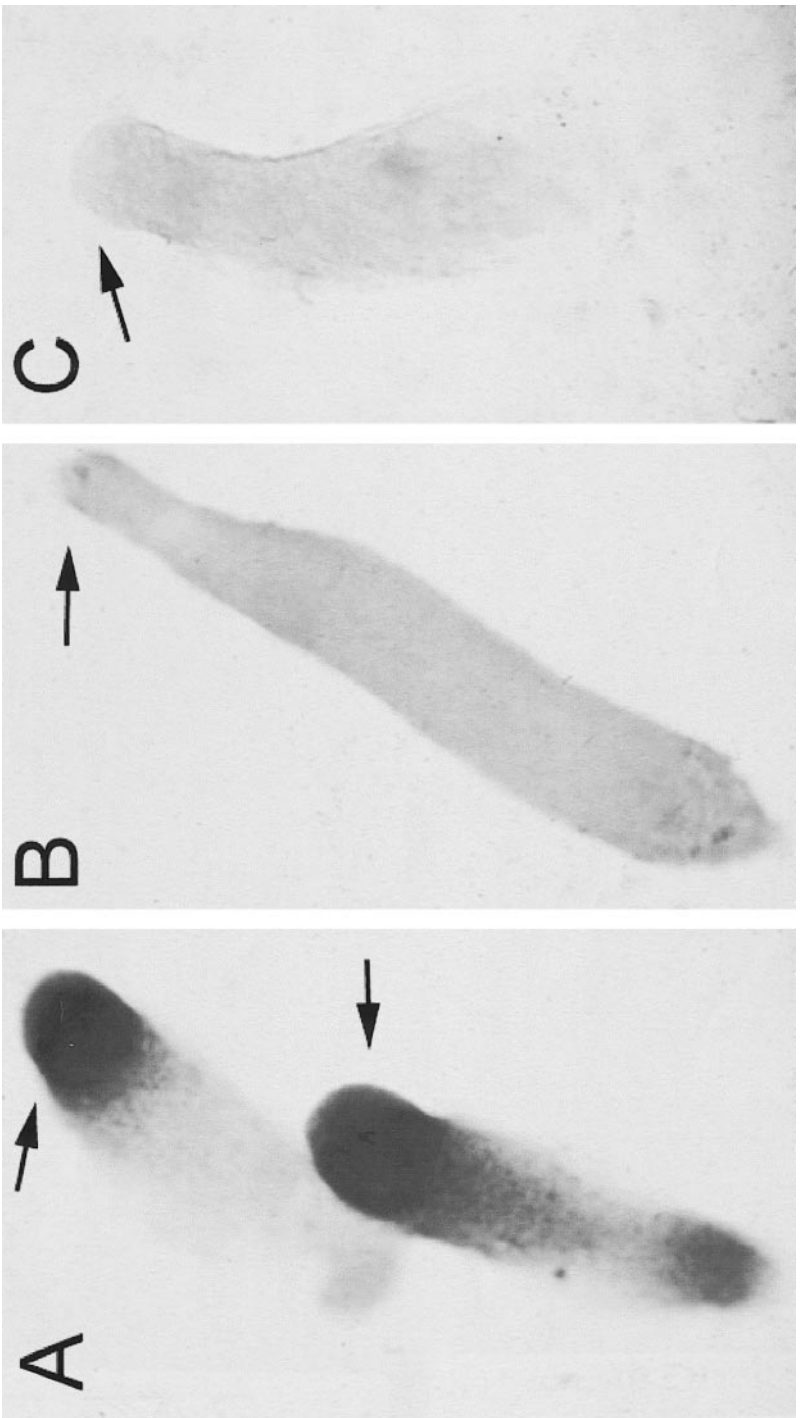

FIG. 2. Expression pattern of *fbxA* in slugs as determined by *in situ* hybridisation analysis. Arrows mark the anterior of the slugs. The dUTP digoxigenin-labeled riboprobes were transcribed from a plasmid (316 MN) containing 175 bp PCR-amplified from the extreme N-terminus of the *fbxA* coding region (see Materials and Methods for exact details of plasmid construction and probe synthesis). (A) Parental Ax2 slugs, probed with an antisense probe. (B) *fbxA*$^-$ slugs, probed with an antisense probe. (C) Parental Ax2 slugs, probed with a control, sense probe.

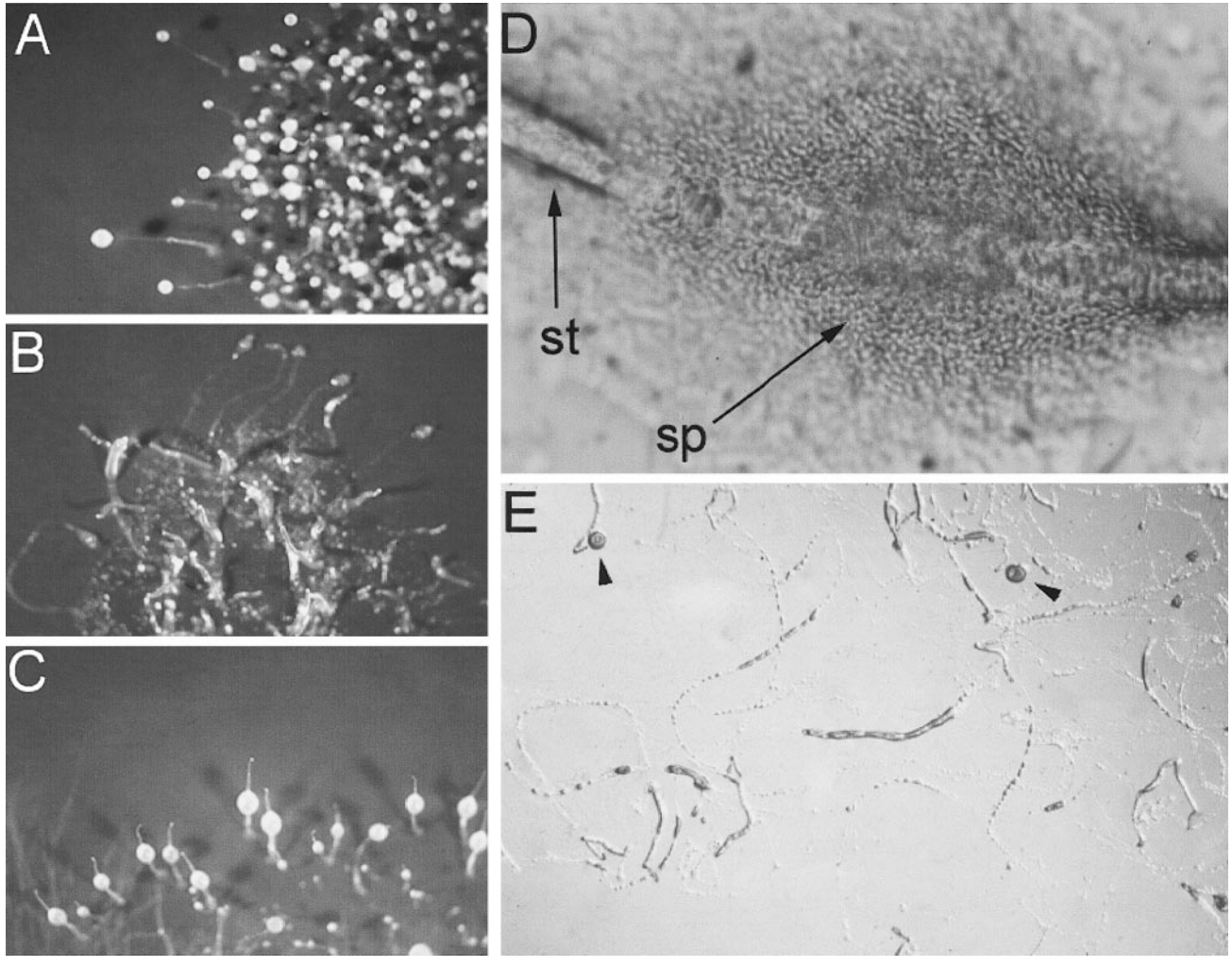

FIG. 3. The *fbxA*$^-$ phenotype. In A–C cells were developed on nitrocellulose filters and in D and E they were developed on agar. (A) Fruiting bodies formed by the parental Ax2 strain in unidirectional (tangential) light. Note that the spore heads are completely raised up the stalks (most easily seen in structures to the left). Identical structures are formed when Ax2 cells are developed under overhead light. (B) Migratory *fbxA*$^-$ slugs after 14 h of development under overhead light. Note the slime trails left behind as the slugs migrate away from the area of original cell deposition. Ax2 cells developed under similar conditions proceed directly from first finger formation into culmination. (C) Terminal morphology of *fbxA*$^-$ cells upon development under overhead light. Note that the spore masses are only partially raised up the stalk. (D) High-powered view of an *fbxA*$^-$ culminant (such as those in C), showing the stalk (st) and sporehead (sp). Note the thick wall of the stalk tube and the honeycomb-like, vacuolated stalk cells inside. The spores are the individual ellipsoid cells within the sporehead. Note that the stalk tube can also be seen passing through the spore mass, showing that the culminant is formed by the normal "reverse fountain" movement of the prestalk cells. (E) *fbxA*$^-$ slugs after prolonged migration on water agar. Samples were incubated for 60 h in unidirectional light followed by exposure to overhead light for an additional 3 days. Note the extensive shedding of cells in the slime trails and the mound-like terminal structures formed in some cases (marked by arrowheads).

to the inhibitory effects of ammonia than their respective parental strains (Fig. 4). Ax2 cells form normal culminants at concentrations of NH_4Cl up to 60 mM (Fig. 4G) and can form small culminants at 75 mM NH_4Cl (Fig. 4I). In contrast, the already low efficiency of *fbxA*$^-$ culmination at 0, 5, and 10 mM NH_4Cl (data not shown and Fig. 4B) is further decreased at 20 and 40 mM NH_4Cl (Figs. 4D and 4F). *fbxA*$^-$ cells arrest as tight mounds at 60 mM NH_4Cl (Fig. 4H) and fail to even aggregate at 75 mM NH_4Cl (Fig. 4J).

fbxA$^-$ *Slugs Are Aberrant in Cell-Type Proportioning*

We next determined the developmental potential of *fbxA*$^-$ cells using cell-type-specific markers. The *pspA* gene is selectively expressed in prespore cells (Early *et al.*, 1988) and the *pspA:gal* reporter construct contains the promoter of *pspA* fused to *lac*Z. In first fingers formed by Ax2 cells transformed with *pspA:gal*, the prespore region is stained and there are a few scattered staining cells in the prestalk region (Fig. 5A). In comparison, the *fbxA*$^-$ structures show a larger prespore region (Fig. 5B); although somewhat variable in its precise length, the stained region in *fbxA*$^-$ first fingers is consistently longer, relative to the total length of the slug, than that observed in Ax2 slugs. Similar results were obtained with the prespore-specific gene *SP60/cotC* (data not shown). In order to confirm that this altered staining pattern reflects a change in the number of prespore cells, parental and *fbxA*$^-$ slugs were dissociated and the constituent cells were analysed either using a monoclonal antibody directed against pspA or using cells transformed with the *SP60:gal* reporter (in conjunction with histochemical staining). The *fbxA*$^-$ slugs contain an increased proportion of pspA-gal and SP60:gal-expressing cells, with slightly over 10% more prespore cells in the mutant slug cells (0 h in Table 1; data not shown for SP60:gal). This difference increases after further slug migration to reach a plateau value (10 h and 24 h in Table 1).

The *ecmAO:gal* marker contains the entire promoter of the *ecmA* gene fused to *lac*Z (Early *et al.*, 1993). It is expressed in pstA cells, in pstO cells, and in ALC. In parental cells analysed at the first finger stage, the approximate front one-fifth is stained and there are scattered stained cells in the prespore region (Fig. 5C). In *fbxA*$^-$ cells the prestalk region is significantly reduced in size relative to the parental strain (Fig. 5D). Again, there is some variability from slug to slug, but the average size of the prestalk region is clearly reduced and the extent of the reduction correlates well with that expected from the increase in the prespore domain (Fig. 5B).

We next determined which of the prestalk populations is aberrant in the mutant. The *ecmO:gal* reporter construct contains a cap site distal subfragment of the promoter of the *ecmA* gene fused to *lac*Z (Early *et al.*, 1993). *ecmO:gal* is expressed in the pstO cells, which form a band in the posterior part of the prestalk region, and also in ALC (Fig. 5E). The pstO band is narrower in *fbxA*$^-$ mutant slugs than is the case for parental first fingers (Fig. 5F), but the size of the unstained anterior, pstA, region appears approximately similar. The unaltered size of the pstA region in the *fbxA*$^-$ mutant was also confirmed directly using *ecmA:gal*, the reporter specific for pstA cells (data not shown). We confirmed these whole-mount results using dissociated samples. There is no statistically significant difference between the pstA population sizes of fbxA and parental slugs but the proportion of pstO cells is significantly smaller in the mutant strain (Table 2).

We conclude, therefore, that slug formation in the *fbxA*$^-$ mutant is aberrant. There is a higher proportion of prespore cells and this is at the expense of the pstO population, with the size of the pstA population remaining approximately normal.

Overexpression of FbxA Reduces the Size of the Prespore Region

The above data suggest that FbxA is necessary for generating and maintaining the correct ratio of prestalk to prespore cells. It was therefore of interest to determine the effect of overexpressing FbxA. The *fbxA* gene was placed under control of the semiconstitutive *actin15* promoter. A FLAG epitope tag was included at the C-terminus of FbxA and the construct was transformed into *Dictyostelium* cells using G418 as selectable marker. Western blot analysis shows that a protein of the predicted size is expressed (Fig. 6A) and that increasing the concentration of G418 used in the selection increases expression of the fusion protein (compare lanes marked G20 with those marked G100). No such band is observed in untransformed cells (Fig. 6A). First fingers formed from cells selected at 100 μg/ml G418 were fixed and stained with a polyclonal antibody specific to prespore cells (Hayashi and Takeuchi, 1976). The first fingers derived from FbxA-FLAG overproducers show a marked reduction in the size of the prespore region relative to the parental strain (Figs. 6B and 6C). This difference was confirmed by dissociating first fingers and staining with a monoclonal antibody directed against the pspA protein. In contrast to the approximately 70% staining observed for wild-type cells (Table 1), only 60% of the cells from the overproducer were stained (*N.B.* Because both the FbxA overexpression construct and the cell-type-specific reporters are carried on G418 resistance plasmids, it was not readily possible to study prestalk cell differentiation). In order to determine whether there is a corresponding increase in the size of the prestalk zone in first fingers derived from overproducing cells, *in situ* analysis was performed using an *ecmA* probe. As expected, expression of the *ecmA* gene was detected in both the pstA and the pstO region of wild-type and mutant structures (Figs. 6D and 6E). However, the size of the prestalk region is noticeably larger in the mutant structures relative to that observed in the parental strain. Thus, whereas the prespore:prestalk ratio increases in the absence of FbxA protein, this ratio decreases when FbxA is overexpressed.

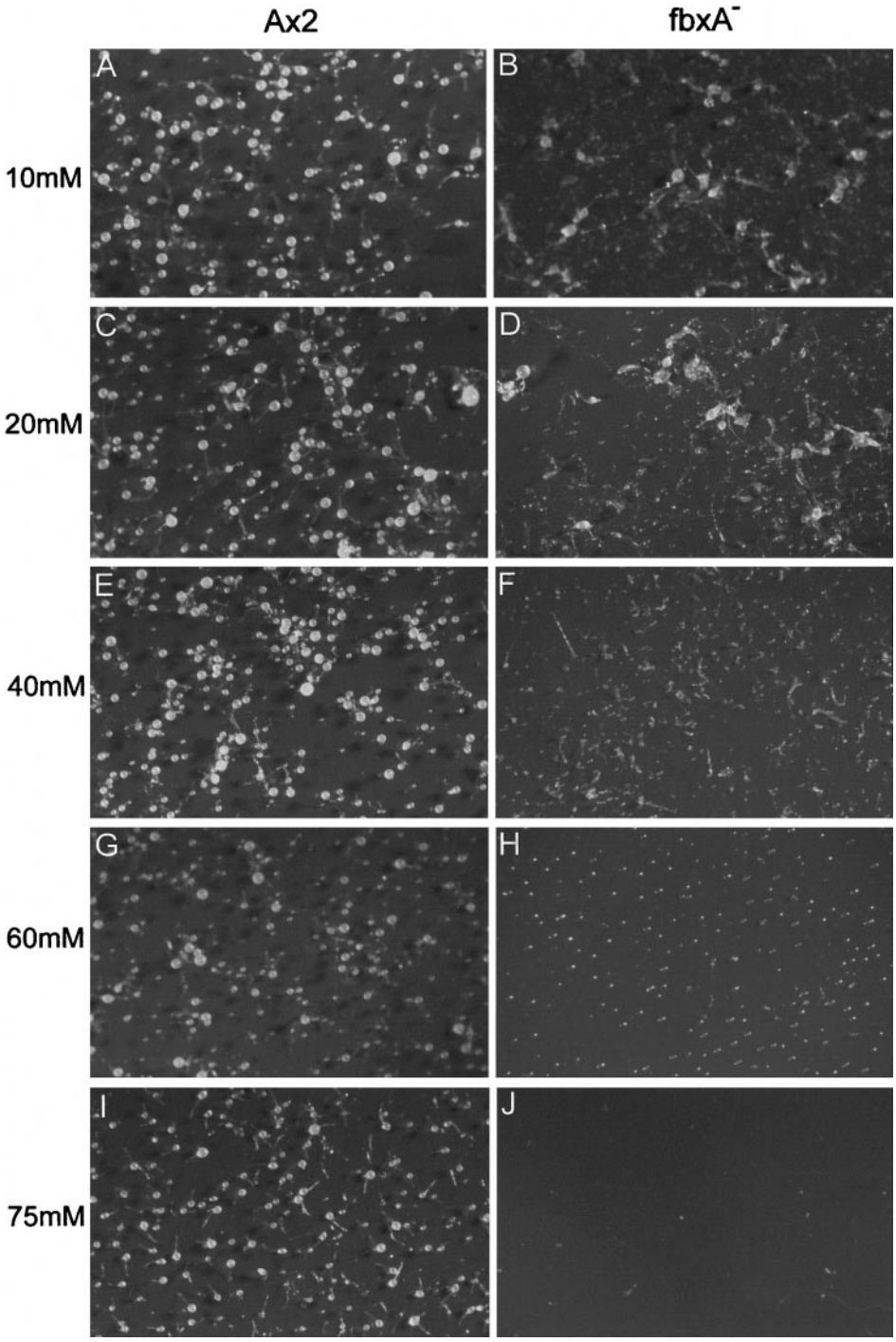

FIG. 4. Ammonia hypersensitivity assay. Ax2 and *fbxA*$^-$ cells were developed under overhead light in the presence of 25 mM MES, pH 6.2, and varying concentrations of ammonium chloride. Cells were plated on nitrocellulose filters at a density of 2.5×10^6 cells/cm^2. The photographs show the terminal morphology, following 46 h of incubation under these conditions. Note that similar results were obtained with *fbxA1*$^-$ cells when compared to the *DH1* parent; the plating density used in that case was 5.0×10^6 cells/cm^2. A, C, E, G, and I show Ax2 cells. *fbxA2*$^-$ cells are shown in B, D, F, H, and J. (A and B) 10 mM NH_4Cl; (C and D) 20 mM NH_4Cl; (E and F) 40 mM NH_4Cl; (G and H) 60 mM NH_4Cl; (I and J) 75 mM NH_4Cl.

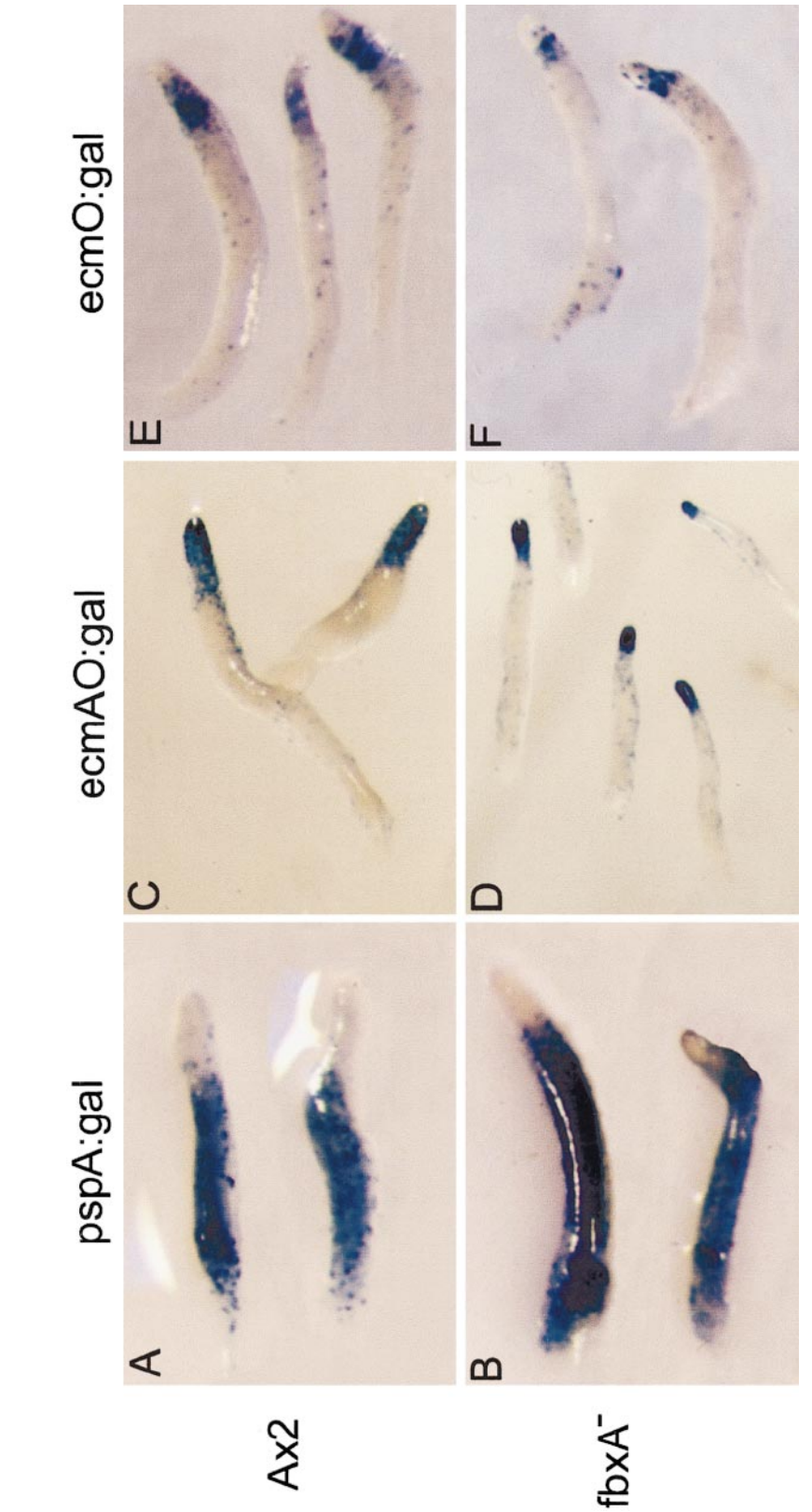

FIG. 5. Pattern formation in *fbxA*$^-$ and wild-type first fingers. Ax2 and *fbxA*$^-$ cells, transformed with one of a series of cell-type-specific *lacZ* reporter constructs, were developed to the first finger stage and stained for β-galactosidase activity. A, C, and E show Ax2 structures. *fbxA*$^-$ structures can be seen in B, D, and F. A and B show the expression pattern of the prespore-specific expression construct *pspA:gal*. C and D show the staining pattern for the prestalk-specific reporter *ecmAO:gal*. Structures derived from *ecmO:gal* transformants are shown in E and F. *ecmO:gal* is specifically expressed in pstO cells and ALC. The unstained region in the very anterior of the slugs consists of pstA cells. Structures A–D are derived from pooled populations, while E and F are derived from the cloned cells used in the experiment described in Table 2. Pooled populations did however also give identical results to those shown in E and F.

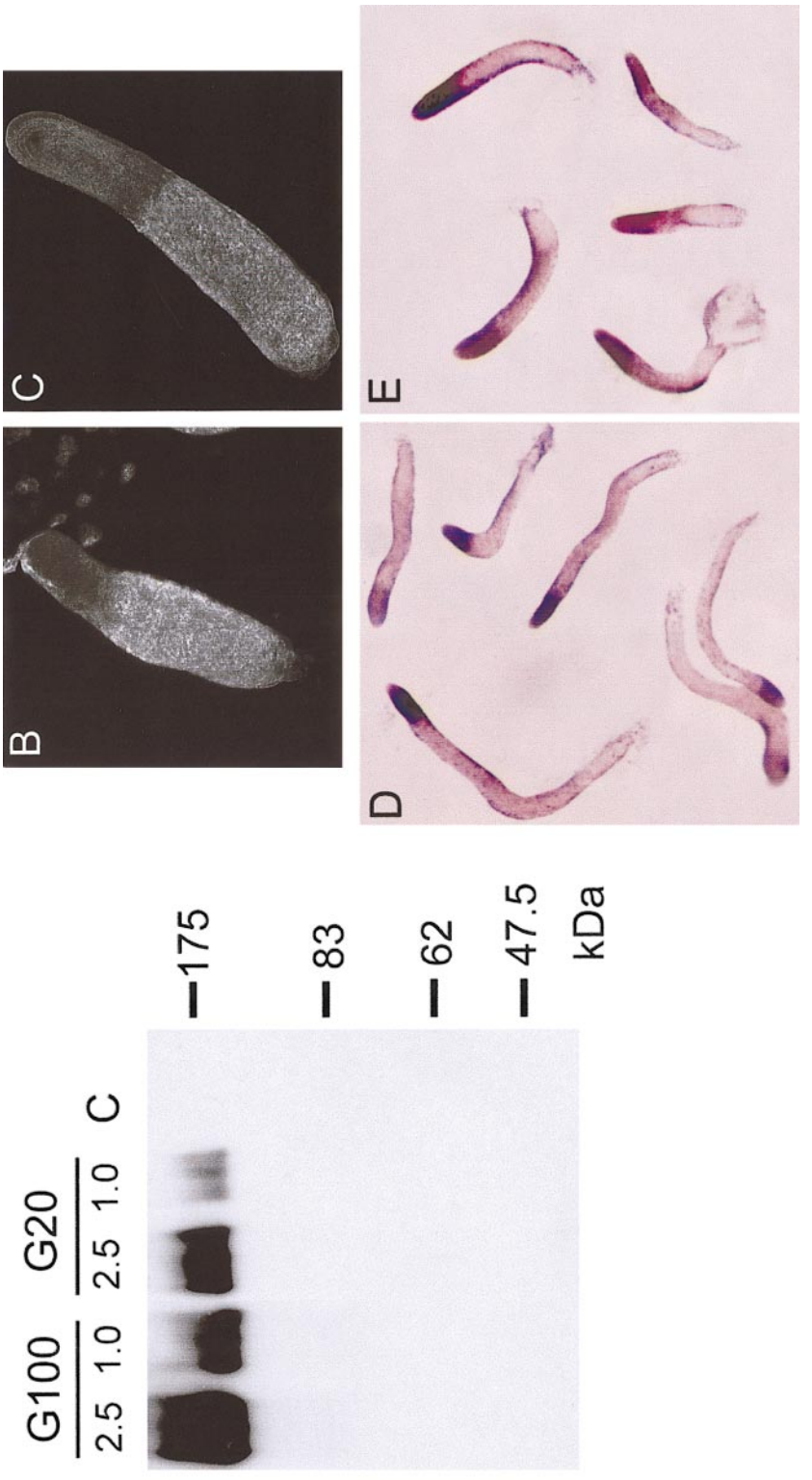

FIG. 6. Analysis of FbxA overexpression. (A) Western blot analysis of *actin15*-FbxA-FLAG transformants. Ax2 cells were transformed with the *actin15*-FbxA-FLAG construct F2 (see Materials and Methods). The original transformation pool was selected at 20 μg/ml G418 (G20). A derivative population was later established at 100 μg/ml G418 (G100). Cell extracts were prepared from transformants and subjected to Western blot analysis, using a polyclonal anti-FLAG antibody. Two sample volumes (2.5 and 1.0 μl) were loaded for extracts from both G20 and G100 cells. Note the prominent band present in all lanes, except C (negative control lane, containing 5.0 μl cell extract prepared from untransformed Ax2 cells). The expected size of the FbxA-fusion protein is approximately 143 kDa. The migration distance of molecular weight standards is shown to the right of the blot. Similar results were obtained from a parallel transformation with the *actin15*-FbxA-FLAG plasmid F5 (data not shown; see Materials and Methods for explanation of F5's origin). B and C show whole mounts of first fingers stained with a polyclonal antibody specific to prespore cells (Hayashi and Takeuchi, 1976). The prestalk region can be dimly seen in the upper portion of each frame. The structures were formed from either Ax2 cells (B) or Ax2 cells transformed with *actin15*-FbxA-FLAG and selected at 100 μg/ml G418 (C). D and E show expression pattern of *ecmA* marker in slugs as determined by *in situ* hybridisation analysis. The dUTP digoxigenin-labeled riboprobes were transcribed from a plasmid containing 800 bp PCR-amplified from the N-terminus of the *ecmA* coding region (kind gift provided by N. Oswald and C. J. Weijer). Parental Ax2 slugs (D). Ax2 cells transformed with *actin15*-FbxA-FLAG and selected at 100 g/ml G418 (E).

TABLE 1

Percentage of Prespore Cells in Parental, *fbxA*$^-$ and FbxA Overexpressor Slugs

Strain	Duration of migration		
	0 h	10 h	24 h
fbxA$^-$	81.5% (SD 2.4%, $n = 6$)	91.2% (SD 2.36%, $n = 3$)	92.1% (SD 1.53%, $n = 3$)
Ax2	70.3% (SD 2.9%, $n = 5$)	75.6% (SD 3.81%, $n = 3$)	77.8% (SD 3.74%, $n = 3$)
FbxA++	60.2% (SD 3.4%, $n = 8$)	n.d.	n.d.

Note. Structures formed by cells from the indicated strains were disaggregated at varying times during development (first finger or after 10 or 24 h of slug migration), by passage through a 23-gauge needle, and stained with the Mud1 antibody, which is specific for the prespore protein pspA. Fields were chosen at random and the percentage of total cells stained was determined. The FbxA++ entry denotes cells expressing the FbxA-FLAG construct. n.d., not determined.

In Synergy Experiments with the Parent Strain, fbxA$^-$ *Cells Are Progressively Excluded from the Prestalk Region and from the Front of the Prespore Zone*

A valuable method of comparing the developmental potential of two different strains is to study their relative behaviours in chimeric structures. *fbxA*$^-$ mutant cells and their respective parental strains were marked by transformation with an *actin15-lacZ* construct. Because the *actin15* promoter is expressed in all cell types (Knecht *et al.*, 1986), transformed cells stain regardless of cell type and location. Mixtures that consisted of 10% marked cells and 90% unmarked cells were allowed to develop and then stained to reveal the location of cells containing β-galactosidase. Staining patterns of synergized structures reveal a clear effect of the *fbxA* mutation on cell localization. In slugs that have migrated for 3 h, containing a mixture of 10% marked mutant and 90% unmarked parental cells, the mutant cells show a marked preference for the rear of the prespore and prestalk regions (Fig. 7A). Conversely, in mixtures where the marked cells are parental and the unmarked cells are mutant, the parental cells show a preference for the anterior of the prespore and prestalk regions (Fig. 7B). Synergized slugs allowed to undergo prolonged migration in unidirectional light show an even more dramatic difference in parental and mutant cell distribution. In slugs in which the mutant population is marked, staining is entirely confined to the very rear of the prespore region (Fig. 7C). In contrast, in slugs where 90% of cells are mutant, the marked parental cells are located exclusively in the tip (Fig. 7D).

Initial Events in Culmination of fbxA$^-$ *Slugs Appear Relatively Normal If There Is No Slug Migration*

We next analysed culmination to determine how an alteration in cell-type proportioning affects terminal morphogenesis. An initial event in terminal stalk-cell differentiation is the activation of *ecmB* expression. This event occurs sporadically during slug migration in a subset of the pstA cells located near the tip; these cells activate *ecmB* expression and a forward facing cone of pstAB cells is produced. Selective staining with a vital dye shows that the cells composing this cone are periodically shed from the back of the slug (Sternfeld, 1992). They are replaced by the redifferentiation of pstA cells. The *ecmB:gal* reporter, which contains the entire *ecmB* promoter fused to *lac*Z, was transformed into parental and *fbxA*$^-$ cells. A cone of pstAB cells is present in young slugs formed by both Ax2 and *fbxA*$^-$ cells. (Figs. 8A and 8B). As *fbxA*$^-$ slugs migrate, the cone of stained pstAB cells sometimes seems to become larger than in the parent strain but it is difficult to quantitate this difference because the size of the pstAB cone is highly variable in parental slugs.

Although *fbxA*$^-$ slugs have an aberrant ratio of pstO to prespore cells, they can form fruiting bodies if they are induced to culminate without prolonged migration by exposing them to overhead light. We therefore analysed the early stages of culmination using the *ecmB:lacZ* reporter. At culmination this reporter is activated in pstA cells as they enter the stalk tube and in the cells that compose the upper and lower cups and the outer basal disc. Differentiation of the lower cup and the outer basal disc seems to be normal in the *fbxA*$^-$ strain (data not shown). The upper cup is believed to derive in part from pstO cells that differentiate *in situ* and in part from ALC that move to the apex of the spore mass (Jermyn and Williams, 1991). It is therefore of particular interest to analyse upper cup cell differentiation, because *fbxA*$^-$ slugs are deficient in pstO cells. At early stages of culmination there is a band of upper cup cells in the *fbxA*$^-$ culminants that is of the same approximate

TABLE 2

Percentage of pstA and pstO Cells in Parental and *fbxA*$^-$ Slugs

Strain	PstA cells	PstO cells
Ax2	5.2% (SD 2.6%, $n = 5$)	18.4% (SD 2.9%, $n = 5$)
fbxA$^-$	3.7% (SD 2.2%, $n = 6$)	12.5% (SD 1.8%, $n = 5$)

Note. Structures formed by cells expressing an *ecmA:gal* fusion gene or an *ecmA:gal* fusion gene, i.e., fusion genes containing the *ecmA* promoter regions that respectively direct expression in pstA and pstO cells, were disaggregated at the first finger stage by passage through a 23-gauge needle. Fields were chosen at random and the percentage of total cells stained was determined.

size as that observed in the parental strain (Figs. 8C and 8D). Hence, it appears that upper cup formation is initiated normally. No upper cup is visible at the top of *fbxA*$^-$ spore masses in final culminants but by this stage the spore head is far below the apex of the stalk (Figs. 8E and 8F). The *fbxA*$^-$ culminants do have a heavily stained thickened region (marked with an arrowhead in Fig. 8F), at the apex of the stalk, which perhaps contains the cells that would normally have composed the upper cup. Perhaps, therefore, the upper cup of *fbxA*$^-$ culminants remains physically linked to the ST cells when the spore mass separates from the apex of the stalk.

After prolonged slug migration, *fbxA*$^-$ mutants are unable to enter culmination but, upon exposure to light, some slugs form misshapen mounds of cells (Fig. 3E). We were interested in determining whether these terminal structures showed any evidence of *ecmB:lacZ staining* reminiscent of early culminants. In most cases (see left-hand structure in Fig. 8G), only scattered staining is observed. Occasionally, however, an additional short, stalk-like, stained region is seen (right-hand structure in Fig. 8G).

DISCUSSION

FbxA is necessary for correct cell-type specification; first fingers and slugs derived from *fbxA*$^-$ mutant cells contain an excess of prespore cells and a reduced number of pstO cells, while the proportion of pstA cells remains approximately normal. Conversely, overexpression of FbxA leads to a reduction in the prespore population and an apparent increase in the prestalk population. The defect in pstO cell formation in the null cells may relate to the characteristic structure of the fruiting body that is formed. Previous work has shown that the upper cup acts to lift the spore head up the stalk at culmination (Sternfeld, 1998). The upper cup in part derives from the pstO cells (Jermyn and Williams, 1991), so a deficit of pstO cells could perhaps lead to defective spore elevation. However, at the late stages of culmination, it was not possible to determine whether the *fbxA*$^-$ mutant has a deficit of upper cup cells.

We do not know why there should be an increase in prespore differentiation at the expense of prestalk differentiation, but the nature of the results argue against one, simplistic model. PstA and pstO differentiation are both induced by DIF, and DIF also acts to repress prespore differentiation. Any change in the sensitivity to DIF could therefore, in principle, shift the balance between prestalk and prepore cell differentiation. However, it seems very unlikely that *fbxA*$^-$ cells have a decreased sensitivity to DIF because pstA differentiation is normal in the mutant, and pstA cell differentiation requires a 10 times *higher* DIF concentration than pstO cell differentiation (Early *et al.*, 1995).

One potentially important piece of information in understanding the *fbxA*$^-$ phenotype is the extent to which the defect is cell autonomous. In synergy experiments, where *fbxA*$^-$ cells are codeveloped with an excess of wild-type cells, the *fbxA*$^-$ cells initially populate the prestalk and prespore zones. However, the *fbxA*$^-$ cells are enriched in the rear part of both regions. After a period of slug migration, this rearward accumulation becomes even more pronounced and the *fbxA*$^-$ cells become entirely concentrated at the back of the prespore region. The fact that the *fbxA*$^-$ cells are initially present both within the prestalk and prespore zones suggests that they are not entirely aberrant in initial differentiation when developing in the presence of a large excess of parental cells. However, their subsequent behaviour can be interpreted in a number of ways. There could, for example, be a defect in the process of prestalk cell replenishment in the mutant cells. Parental cells in a predominantly mutant background would then be preferentially recruited to the tip, to replenish the prestalk population after its depletion during migration. Conversely, mutant cells in a slug composed largely of parental cells would be less likely to take on anterior fates during migration. The fact that the percentage of prespore cells in *fbxA*$^-$ slugs increases upon prolonged migration (Table 1) is consistent with this model. However, there are alternative explanations. For example, the pstA, pstO, and prespore populations in a normal slug differ in relative rates of chemotaxis to cAMP: the pstA cells move slightly faster than the pstO cells and the prespore cells move much slower than either prestalk population (Abe *et al.*, 1994). The *fbxA*$^-$ cells might therefore have a general reduction in mobility relative to the parental cells, so that each mutant pstO, pstA, and prespore cell type moves more slowly than its wild-type counterpart.

Null mutations in the *fbxA* gene also have several effects upon late development that seem likely to be linked in some way. There is, for example, a well-established correlation between ammonia hypersensitivity and an increased propensity for slug migration (Gee *et al.*, 1994) and the *fbxA*$^-$ strain shows both these properties. Entry into culmination is regulated by cAMP dependent protein kinase (Harwood *et al.*, 1992; Mann *et al.*, 1992) and recently a pathway that links ammonia to production of intracellular cAMP via a sensor histidine kinase has been proposed (Singleton *et al.*, 1998). It will be of interest to see whether the *fbxA*$^-$ strain has altered levels of any of the proteins in this pathway.

Analysis of the predicted protein sequence reveals that FbxA is a member of a growing family of proteins that contain an F-box upstream of a series of WD40 repeats. According to the "F-Box Hypothesis," the WD40 repeats interact with specific protein(s) targeted for ubiquitin-mediated degradation and the F-box domain interacts with the cellular ubiquitination machinery (Bai *et al.*, 1996; Patton *et al.*, 1998; Maniatis, 1999). Of particular interest in this context are several F-box proteins recently shown to regulate cell fate decisions and pattern formation in *Dictyostelium*, plants, and metazoans. Function of a *Dictyostelium* MEK kinase, MEKKα, is regulated by ubiquitination. In addition to its kinase domain, MEKKα contains

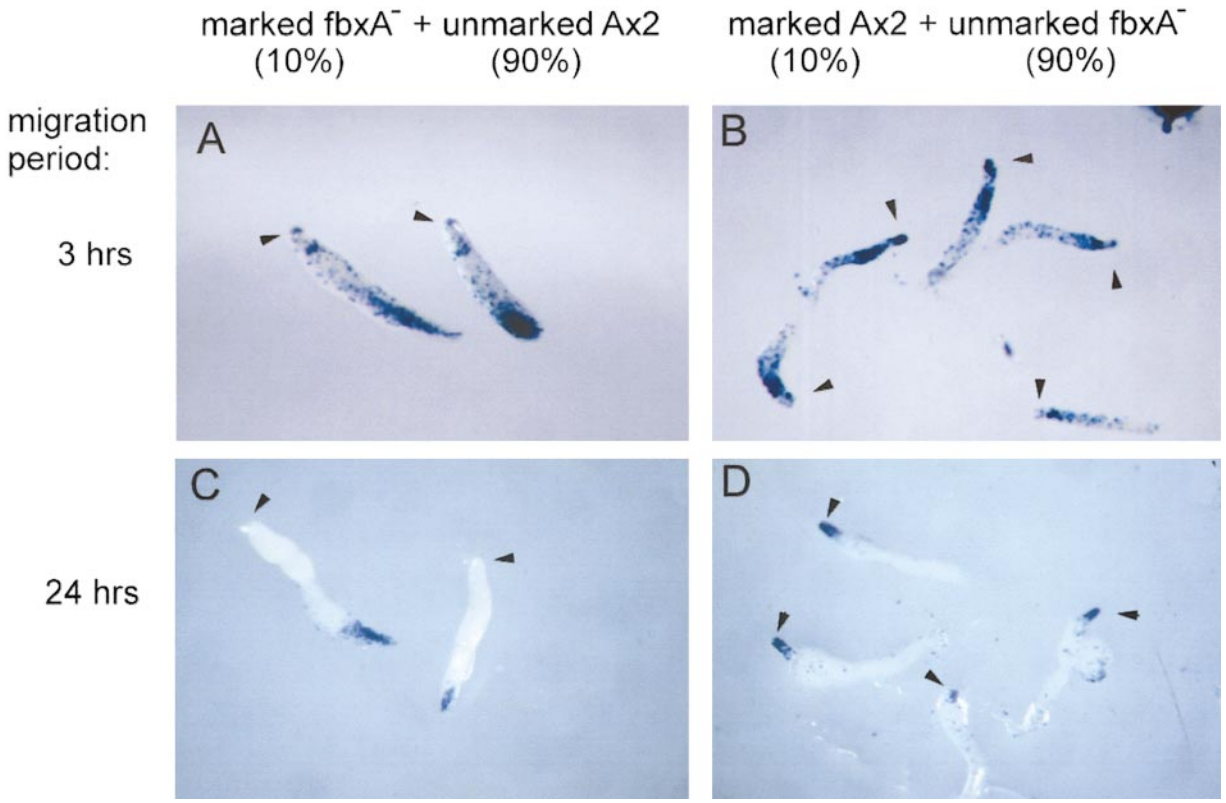

FIG. 7. Staining pattern of chimeric slugs. Ax2 and *fbxA*⁻ cells were transformed with *actin15-lacZ*, a marker that is expressed in all cell types. Chimeric structures consisting of 10% marked cells and 90% unmarked cells were prepared by mixing cells immediately prior to development. The resulting slugs were allowed to migrate for either 3 h (A and B) or 24 h (C and D) before fixation and staining. In A and C the mutant cells are the marked population. Ax2 cells are marked in B and D. Arrowheads indicate the anterior of the slugs. In order to determine whether the marking process per se had any effect on the developmental fate of the cells, control experiments were also carried out in which both the marked and the unmarked populations were of the same genotype (both Ax2 or both *fbxA*⁻). Stained cells were distributed evenly throughout these control slugs (data not shown).

both an F-box and WD40 repeats that mediate its interaction with the ubiquitination machinery (Chung *et al.*, 1998). *Mekkα* null strains or strains overexpressing a dominant negative MEKK*α* form slugs with an increased proportion of pstO cells and a concomitantly decreased proportion of prespore cells (Chung *et al.*, 1998). Conversely, cells overexpressing wild-type MEKK*α* show increased prespore differentiation and decreased pstO differentiation. MEKK*α* stability is spatially and temporally regulated by the ubiquitin-conjugating enzyme UBC1, which directs degradation, and the deubiquitinating enzyme UCP1, which stabilizes MEKK*α*. Mutants lacking UBC1 contain an excess of pstB cells and are impaired in both tip formation and culmination (Clark *et al.*, 1997). Disruption of the *nosA* gene, which encodes NOSA, another component of the ubiquitination machinery, results in developmental arrest following aggregation (Pukatzki *et al.*, 1998).

In plants, the FIM (fimbritia) protein of *Antirrhinum* and UFO (Unusual Floral Organs) gene of *Arabodopsis* are closely related F-box/WD40 proteins that regulate floral homeotic genes (Ingram *et al.*, 1995). For example, *fim*⁻ mutants show decreased message levels of the MADS box transcription factor *deficiens*, suggesting that FIM normally mediates degradation of an inhibitor of *deficiens* expression (Ingram *et al.*, 1997). In *C. elegans*, the F-box/WD40 protein SEL-10 negatively regulates activity of the lin-12/Notch pathway, apparently via interaction with the intracellular domain of the lin-12/Notch receptor itself (Hubbard *et al.*, 1997). In *Drosophila*, absence of the F-box/WD40 protein Slimb results in ectopic activity of genes responsive to the Hedgehog and Wingless signaling pathways (Jiang and Struhl, 1998). Slimb is also required for activation of dorsal, the *Drosophila* NF-κB homologue (Spencer *et al.*, 1999). Nuclear localization of dorsal, which occurs in response to activation of the Toll-receptor signaling pathway, requires ubiquitin-mediated degradation of the Iκ-B homologue cactus (reviewed in Morisato and Anderson, 1995). Interestingly, the vertebrate homologue of Slimb, β-TrCp, has been implicated in ubiquitin-mediated degradation of Iκ-B, β-catenin (a component of the Wingless signaling pathway), and CD-4 (as a consequence of HIV infection) (Margottin *et al.*, 1998; Yaron *et al.*, 1998; Spencer *et al.*, 1999; Winston *et*

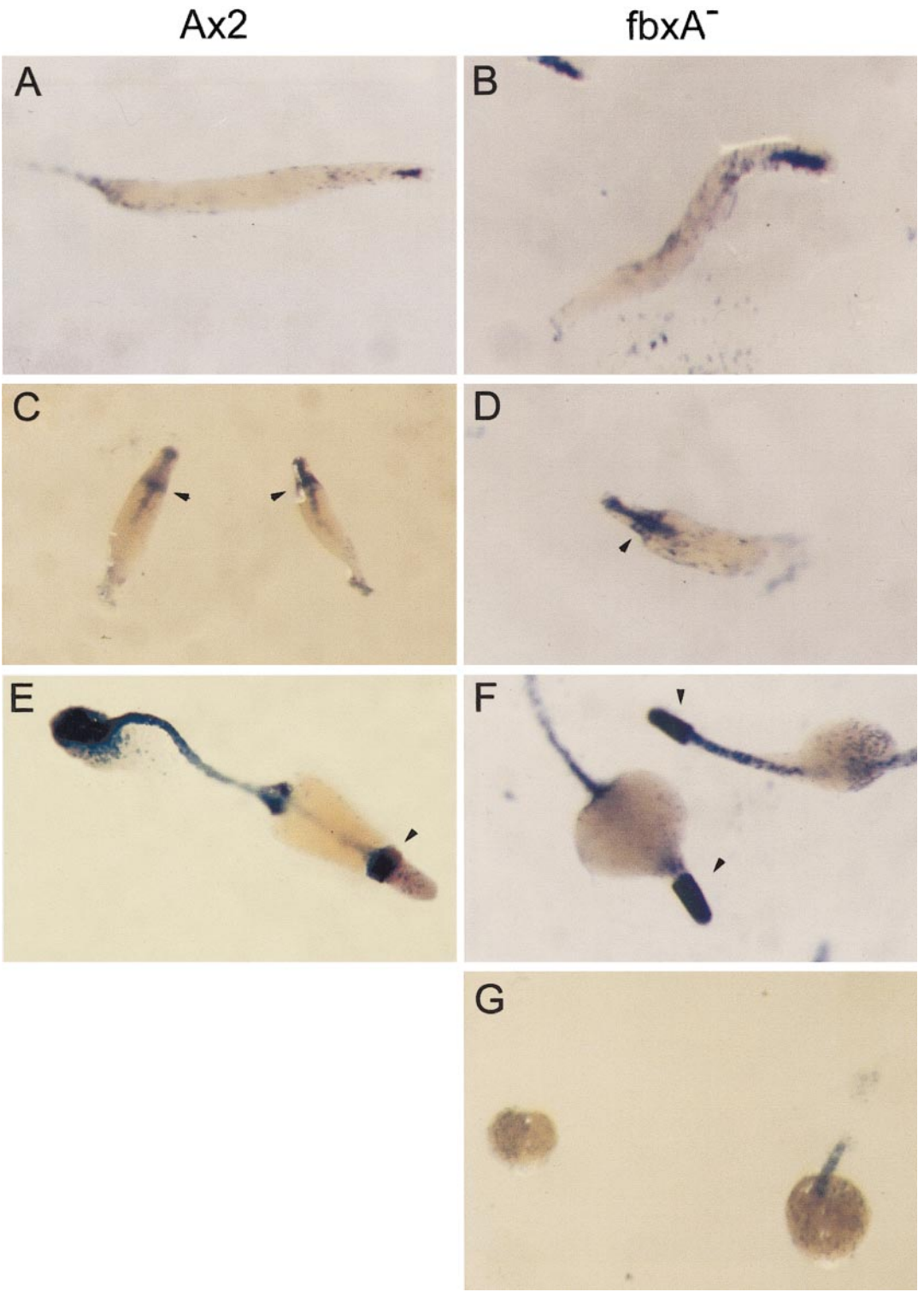

FIG. 8. *ecmB:gal* expression patterns. Ax2 and *fbxA*$^-$ cells were transformed with the ecmB:gal reporter. Whole mounts of the resulting transformants, fixed and stained at various stages of development, are shown. A and B show young Ax2 and *fbxA*$^-$ slugs, respectively. Note the conical region of staining in the slug tip. Early preculminants formed by Ax2 (C) and *fbxA*$^-$ (D) cells both show a similar region of upper cup staining (indicated by arrowheads). A stalk tube can also be seen in the upper one-third to one-half of the structures. E and F show culminants from Ax2 and *fbxA*$^-$ cells, respectively. In contrast to the normal upper cup structure seen in E, mutant structures have no staining at the apex of the spore mass. However, a thickened region of intense staining is observed at the top of the stalk (marked with arrowheads in F). Two different stages in the *fbxA*$^-$ culmination process are shown in F. The lower left-hand structure shows an intermediate stage, at which the spore mass is still near to the top of the forming stalk. As development proceeds, the spore mass separates from the top of the stalk, and the stalk continues to extend upward, until the final aberrant culminant is produced (upper right-hand structure). G shows the amorphous mounds produced when *fbxA*$^-$ slugs are exposed to light after prolonged migration. See also the structures marked with an arrowhead in Fig. 3E.

al., 1999; reviewed in Maniatis, 1999). SEL-10, Slimb, and β-TrCp appear within the top nine matches in a protein homology search in which the entire FbxA amino acid sequence was submitted for comparison.

Although we have no formal evidence that FbxA interacts with the ubiquitination machinery, the presence of the F-box and WD40 repeats strongly suggests that FbxA is differentially regulated by the ubiquitination pathways or functions as a scaffold, like Slimb/β-TrCp, to target other proteins for degradation. Of interest is that both FbxA and MEKKα have null and overexpression phenotypes that affect the ratio of pstO to prespore cells. It is thus possible that these two genes lie on a common genetic pathway. One possible model is that MEKKα acts as a negative regulator of FbxA, where FbxA functions to either promote prestalk differentiation or inhibit prespore differentiation. Identification of components that lie upstream and downstream from FbxA and MEKKα should clarify potential interactions of the proteins and how they regulate cell fate decisions.

ACKNOWLEDGMENTS

The authors thank N. Osherov, W. F. Loomis, H. Ennis, and R. Kessin for sharing unpublished data. This work was supported by The Imperial Cancer Research Fund (M.K.N. and J.G.W.), United States Public Health Service NRSA Grant 51FCA59303-02 (M.K.N.), BBSRC Grant CAD05617 (M.K.N. and J.G.W.), Wellcome Trust Program Grant 050.801709 (T.A. and J.G.W.), and United States Public Health Service Grant GM24279 (R.A.F.). We also thank N. Oswald for kind help with the *in situ* hybridisation analysis.

Accession information and note added in proof. The GenBank Accession number for the genomic sequence of *fbxA* is AF151733. Sequence information (genomic, AF151111; cDNA, AF151112) has been separately submitted (under the name *chtA*). The corresponding locus is called *sokA* in DictyDB (http://probe.nalusda.gov:8300/cgi-bin/browse/dictydb) and in Kuspa and Loomis (1996). Additional *fbxA*$^-$ REMI mutants with plasmid insertions in the same *Dpn*II site as our isolate were independently isolated by N. Osherov and W. F. Loomis (University of California, San Diego) and by H. L. Ennis and R. Kessin and colleagues (Columbia University). After submission of this present paper, the latter group published a description of the gene under the name *chtA* (for Cheater A), because it preferentially forms spores, rather than stalk cells, in synergy experiments (Ennis *et al.*, 2000).

REFERENCES

Abe, T., Early, A., Siegert, F., Weijer, C., and Williams, J. (1994). Patterns of cell movement within the *Dictyostelium* slug revealed by cell type-specific, surface labeling of living cells. *Cell* **77,** 687–699.

Bai, D., Sen, P., Hofman, K. Ma, L., Goebl, M., Harper, J. W., and Elledge, S. J. (1996). SKP1 connects cell cycle regulators to the ubiquitin proteolysis machinery through a novel motif, the F-box. *Cell* **86,** 263–274.

Brown, J. M., Briscoe, C., and Firtel, R. A. (1997). Control of transcriptional regulation by signal transduction pathways in *Dictyostelium* during multicellular development. In "*Dictyostelium*—A Model System for Cell and Developmental Biology" (Y. Maeda, K. Inouye, and I. Takeuchi, Eds.), pp. 245–265. Universal Acad. Press, Tokyo, Japan.

Ceccarelli, A., Mahbubani, H., and Williams, J. G. (1991). Positively and negatively acting signals regulating stalk cell and anterior-like cell differentiation in *Dictyostelium*. *Cell* **65,** 983–989.

Chung, C. Y, Reddy, T. B. K., Zhou, K., and Firtel, R. A. (1998). A novel, putative MEK kinase controls developmental timing and spatial patterning in *Dictyostelium* and is regulated by ubiquitin-mediated protein degredation. *Genes Dev.* **12,** 3564–3578.

Clark, A., Nomura, A., Sudhasri, M., and Firtel, R. A. (1997). A ubiquitin-conjugating enzyme is essential for developmental transitions in *Dictyostelium*. *Mol. Biol. Cell* **8,** 1989–2002.

Dingermann, T., Reindl, N., Werner, H., Hildebrandt, M., Nellen, W., Harwood, A., Williams, J., and Nerke, K. (1989). Optimization and in situ detection of *Escherichia coli* beta-galactosidase gene expression in *Dictyostelium discoideum*. *Gene* **85,** 353–362.

Early, A., Abe, T., and Williams, J. (1995). Evidence for positional differentiation of prestalk cells and for a morphogenetic gradient in *Dictyostelium*. *Cell* **83,** 91–99.

Early, A. E., Gaskell, M. J., Traynor, D., and Williams, J. G. (1993). Two distinct populations of prestalk cells within the tip of the migratory *Dictyostelium* slug with differing fates at culmination. *Development* **118,** 353–362.

Early, A. E., Williams, J. G., Meyer, H. E., Por, S. B., Smith, E., Williams, K. L., and Gooley, A. A. (1988). Structural characterization of *Dictyostelium discoideum* prespore-specific gene D19 and of its product, cell surface glycoprotein PsA. *Mol. Cell. Biol.* **8,** 3458–3466.

Ennis, H. L., Dao, D. N., Pukatzki, S. U., and Kessin, R. H. (2000). *Dictyostelium* amoebae lacking an F-box protein form spores rather than stalk in chimeras with wild type. *Proc. Natl. Acad. Sci. USA* **97,** 3292–3297.

Escalante, R., and Loomis, W. F. (1995). Whole-mount *in situ* hybridization of cell-type-specific mRNAs in *Dictyostelium*. *Dev. Biol.* **171,** 262–266.

Faix, J., Gerisch, G., and Noegel, A. A. (1990). Constitutive overexpression of the contact site A glycoprotein enables growth-phase cells of *Dictyostelium discoideum* to aggregate. *EMBO J.* **9,** 2709–2716.

Francis, D. W. (1964). Some studies on phototaxis of *Dictyostelium*. *J. Cell. Comp. Physiol.* **64,** 131–138.

Fukuzawa, M., Hopper, N., and Williams, J. (1997). cudA: A *Dictyostelium* gene with pleiotropic effects on cellular differentiation and slug behaviour. *Development* **124,** 2719–2728.

Gee, K., Russell, F., and Gross, J. D. (1994). Ammonia hypersensitivity of slugger mutants of D. discoideum. *J. Cell Sci.* **107,** 701–708.

Harwood, A. J., Hopper, N. A., Simon, M. N., Driscoll, D. M., Veron, M., and Williams, J. G. (1992). Culmination in *Dictyostelium* is regulated by the cAMP-dependent protein kinase. *Cell* **69,** 615–624.

Hayashi, M., and Takeuchi, I. (1976). Quantitative analysis on cell differentiation during morphogenesis of the cellular slime mold *Dictyostelium discoideum*. *Dev. Biol.* **50,** 302–309.

Hubbard, E. J. A., Wu, G., Kitajewski, J., and Greenwald, I. (1997). sel-10, a negative regulator of lin-12 activity in *Caenorhabditis elegans*, encodes a member of the CDC4 family of proteins. *Genes Dev.* **11,** 3182–3193.

Ingram, G. C., Goodrich, J., Wilkinson, M. D., Simon, R., Haughn, G. W., and Coen, E. S. (1995). Parallels between unusual floral organs and fimbritia, genes controlling flower development in Arabodopsis and Antirrhinum. *Plant Cell* **7,** 1501–1510.

Ingram, G. C., Doyle, S., Carpenter, R., Schultz, E. A., Simon, R., and Coen, E. S. (1997). Dual roles for fimbritia in regulating floral homeotic genes and cell division in Antirrhinum. *EMBO J.* **16,** 6521–6534.

Jermyn, K. A., and Williams, J. G. (1991). An analysis of culmination in *Dictyostelium* using prestalk and stalk-specific cell autonomous markers. *Development* **111,** 779–787.

Jiang, J., and Struhl, G. (1998). Regulation of the Hedgehog and Wingless signalling pathways by the F-box/WD40-repeat protein Slimb. *Nature* **391,** 493–496.

Kay, R. R. (1997). DIF signalling. In "Dictyostelium—A Model System for Cell and Developmental Biology" (Y. Maeda, K. Inouye, and I. Takeuchi, Eds.), pp. 279–292. Universal Acad. Press, Tokyo, Japan.

Knecht, D. A., Cohen, S. M., Loomis, W. F., and Lodish, H. F. (1986). Developmental regulation of *Dictyostelium discoideum* actin gene fusions carried on low-copy and high-copy transformation vectors. *Mol. Cell. Biol.* **6,** 3973–3983.

Krefft, M., Voet, L., Mairhofer, H., and Williams, K. L. (1983). Analysis of proportion regulation in slugs of *Dictyostelium discoideum* using a monoclonal antibody and a FACS-IV. *Exp. Cell Res.* **147,** 235–239.

Kuspa, A., and Loomis, W. F. (1992). Tagging developmental genes in *Dictyostelium* by restriction enzyme-mediated integration of plasmid DNA. *Proc. Natl. Acad. Sci. USA* **89,** 8803–8807.

Kuspa, A., and Loomis, W. F. (1996). Ordered yeast artificial chromosome clones representing the *Dictyostelium discoideum* genome. *Proc. Natl. Acad. Sci. USA* **93,** 5562–5566.

Maniatis, T. (1999). A ubiquitin ligase complex essential for the NF-κB, Wnt/Wingless, and Hedgehog signaling pathways. *Genes Dev.* **13,** 505–510.

Mann, S. K. O., Yonemoto, W. M., Taylor, S. S., and Firtel, R. A. (1992). DdPK3, which plays essential roles during *Dictyostelium* development, encodes the catalytic subunit of cAMP-dependent protein kinase. *Proc. Natl. Acad. Sci. USA* **89,** 10701–10705.

Margottin, F., Bour, S. P., Durand, H., Selig, L., Benichou, S., Richard, V., Thomas, D., Strebel, K., and Benarous, R. (1998). A novel WD protein, h-βTrCP, that interacts with HIV-1 Vpu connects CD4 to the ER degredation pathway through an F-Box motif. *Mol. Cell* **1,** 565–574.

Morisato, D., and Anderson, K. V. (1995). Signaling pathways that establish the dorsal-ventral pattern of the *Drosophila* embryo. *Annu. Rev. Genet.* **19,** 371–379.

Neer, E. J., Schmidt, C. J., Nambudripad, R., and Smith, T. F. (1994). The ancient regulatory-protein family of WD-repeat proteins. *Nature* **371,** 297–300.

Nellen, W., Silan, C., and Firtel, R. A. (1984). DNA-mediated transformation in *Dictyostelium discoideum:* Regulated expression of an actin gene fusion. *Mol. Cell. Biol.* **4,** 2890–2898.

Newell, P. C., and Ross, F. M. (1982). Genetic analysis of the slug stage of *Dictyostelium discoideum*. *J. Gen. Microbiol.* **128,** 1639–1652.

O'Neill, J. W., and Bier, E. (1994). Double-label in situ hybridization using biotin and digoxigenin-tagged RNA probes. *Biotechniques* **17,** 874–875.

Patton, E. E., Willems, A. R., and Tyers, M. (1998). Combinatorial control in ubiquitin-dependent proteolysis: Don't Skp the F-box hypothesis. *Trends Genet.* **14,** 236–243.

Pukatzki, S., Tordilla, N., Franke, J., and Kessin, R. H. (1998). A novel component involved in ubiquitination in required for development of *Dictyostelium discoideum*. *J. Biol. Chem*. **273,** 24131–24138.

Raper, K. B. (1940). Pseudoplasmodium formation and organization in *Dictyostelium discoideum*. *J. Elisha Mitchell Sci. Soc.* **56,** 241–282.

Schindler, J., and Sussman, M. (1977). Ammonia determines the choice of morphogenetic pathways in *Dictyostelium discoideum*. *J. Mol. Biol.* **116,** 161–169.

Shaw, D. R., Richter, H., Giorda, R., Ohmachi, T., and Ennis, H. L. (1989). Nucleotide sequences of *Dictyostelium discoideum* developmentally regulated cDNAs rich in (AAC) imply proteins that contain clusters of asparagine, glutamine, or threonine. *Mol. Gen. Genet.* **218,** 453–459.

Singleton, C. K., Zinda, M. J., Mykytka, B., and Yang, P. (1998). The histidine kinase dhkC regulates the choice between migrating slugs and terminal differentiation in *Dictyostelium discoideum*. *Dev. Biol.* **203,** 345–357.

Smith, E., and Williams, K. (1980). Evidence for tip control of the "slug/fruit" switch in slugs of *Dictyostelium discoideum*. *J. Embryol. Exp. Morphol.* **57,** 233–240.

Spencer, E., Jiang, J., and Chen, Z. J. (1999) Signal-induced ubiquitination of IκBα by the F-box protein Slimb/β-TrCP. *Genes Dev.* **13,** 284–294.

Sternfeld, J. (1992). A study of pstB cells during *Dictyostelium* migration and culmination reveals a unidirectional cell type conversion process. *Wilhelm Roux's Arch. Dev. Biol.* **201,** 354–363.

Sternfeld, J. (1998). The anterior-like cells in *Dictyostelium* are required for the elevation of the spores during culmination. *Dev. Genes Evol.* **208,** 487–494.

Sutoh, K. (1993). A transformation vector for *Dictyostelium discoideum* with a new selectable marker bsr. *Plasmid* **30,** 150–154.

Watts, D. J., and Ashworth, J. M. (1970). Growth of myxamoebae of the cellular slime mould *Dictyostelium discoideum* in axenic culture. *Biochem. J.* **119,** 171–174.

Winston, J. T, Strack, P., Beer-Romero, P., Chu, C. Y., Elledge, S. J., and Harper, J. W. (1999). The $SCF^{\beta\text{-TRCP}}$-ubiquitin ligase complex associates specifically with phosphorylated destruction motifs in IκBα and β-catenin and stimulates IκBα uquitination in vitro. *Genes Dev.* **13,** 270–283.

Yaron, A., Hatzubai, A., Davis, M., Lavon, I., Amit, S., Manning, A. M., Anderson, J. S., Mann, M., Mercurio, F., and Ben-Neriah, Y. (1998). Identification of the receptor component of the IκBα-ubiquitin ligase. *Nature* **396,** 590–594.

Received for publication March 27, 2000
Revised May 25, 2000
Accepted May 26, 2000